Exchange bias of singly inverted FeO/Fe_3O_4 core-shell nanocrystals

D. W. Kavich and J. H. Dickerson
Department of Physics and Astronomy, Vanderbilt University, Nashville, Tennessee 37235, USA
and Vanderbilt Institute for Nanoscale Science and Engineering, Vanderbilt University, Nashville, Tennessee 37235, USA

S. V. Mahajan and S. A. Hasan
Interdisciplinary Program in Materials Science, Vanderbilt University, Nashville, Tennessee 37235, USA
and Vanderbilt Institute for Nanoscale Science and Engineering, Vanderbilt University, Nashville, Tennessee 37235, USA

J.-H. Park
National High Magnetic Field Laboratory, Florida State University, Tallahassee, Florida 32310, USA
(Received 3 July 2008; revised manuscript received 7 October 2008; published 14 November 2008)

Exchange bias (EB) is investigated in singly inverted FeO/Fe_3O_4 core-shell nanocrystals by vibrating sample magnetometry. A horizontal and vertical shift of the field-cooled (FC) hysteresis loop with respect to the zero-field-cooled (ZFC) hysteresis loop is observed below the blocking temperature of EB ($T_B^{EB} \approx T_N$). An enhancement of the superparamagnetic blocking temperature ($T_B^{SP} \approx 190$ K) with respect to the expected value is observed from the ZFC/FC measurement of $m(T)$. Furthermore, the value of T_B^{SP} is nearly constant for applied fields ranging from 25 to 200 Oe as a result of the exchange coupling at the antiferromagnetic/ferrimagnetic interface.

DOI: 10.1103/PhysRevB.78.174414 PACS number(s): 75.50.Tt, 75.75.+a, 75.70.Cn

I. INTRODUCTION

Exchange bias (EB) coupling at the antiferromagnetic/ferromagnetic (AFM/FM) interface has attracted considerable attention since its discovery by Meiklejohn and Bean[1] in 1956. Numerous applications of EB exist in present technologies, such as spin valves and magnetic tunnel junctions.[2] EB is also being considered as a possible route in overcoming the superparamagnetic limit in magnetic storage media.[3] Review articles on the subject discuss EB in both thin films and core-shell nanocrystals (NCs).[4–6] Most of the research trajectories concerning core-shell NCs have followed the prototypical model of EB set forth by Meiklejohn and Bean in which a FM core is surrounded by an AFM shell, with the Néel temperature (T_N) less than the Curie temperature (T_C). However, variations of the original model are conceivable, such as an inversion of the magnetic structure (an AFM core with a FM shell) or an inversion of the transition temperatures ($T_N > T_C$). Recent interest in the doubly inverted MnO/Mn_3O_4 core-shell system has emerged, since the magnetic structure and transition temperatures are opposite to the original model.[7,8] Here, we report on the singly inverted FeO/Fe_3O_4 core-shell system, which exhibits an inversion of the magnetic structure only.

The basic signature of EB involves a shifted hysteresis loop, usually accompanied by an enhancement of the coercive field after field cooling through T_N of the antiferromagnet. This is a consequence of exchange coupling at the AFM/FM interface, which for parallel coupling tends to stabilize the direction of the FM spins upon reversal of the applied magnetic field. Ohldag *et al.*[9] demonstrated that the magnitude of the exchange field (H_E) directly correlates to the number of uncompensated interfacial spins that are pinned to the antiferromagnet. Enhancement of the coercive field (H_C) is attributed to uncompensated interfacial spins that rotate with the ferromagnet. In general, EB is sensitive to numerous factors, such as interfacial roughness,[10] dimensions of both the antiferromagnet and ferromagnet,[11,12] AFM domain size,[13,14] and AFM anisotropy energy. Note that all of these parameters can affect the number of pinned/unpinned uncompensated spins at the AFM/FM interface.

The FeO/Fe_3O_4 system investigated here consists of a core of FeO (wüstite) surrounded by a shell of Fe_3O_4 (magnetite). Wüstite has a rocksalt crystal structure and is formally written as Fe_xO($x=0.83-0.96$).[15] Furthermore, it undergoes AFM ordering below $T_N \approx 198$ K. At room temperature, magnetite has an inverse cubic spinel structure and undergoes ferrimagnetic (FIM) ordering below $T_C \approx 860$ K.[16] Interaction of the AFM ordering of FeO with the FIM ordering of Fe_3O_4 can result in similar effects as observed in the classic EB system; however, the nature of exchange coupling at the interface is more complicated as a result of the sublattice structure of the ferrimagnet. Nevertheless, the exchange coupling generally results in loop shifts, enhanced coercivity, and an increase in the effective anisotropy energy as typically observed in systems consisting of an AFM/FM interface.

EB of singly inverted FeO/Fe_3O_4 core-shell NCs is probed by vibrating sample magnetometry (VSM). The temperature dependences of H_E and H_C are determined by the zero-field-cooled (ZFC) and field-cooled (FC) measurements of the magnetization $m(H)$. EB is further investigated by measuring the dependence of H_E and H_C on the cooling field (H_{FC}). The weak dependence of the superparamagnetic blocking temperature T_B^{SP} on the applied field is investigated by the ZFC/FC measurement of $m(T)$.

II. NANOCRYSTAL SYNTHESIS

FeO/Fe_3O_4 core-shell NCs are synthesized according to the thermal decomposition of an iron oleate precursor in the

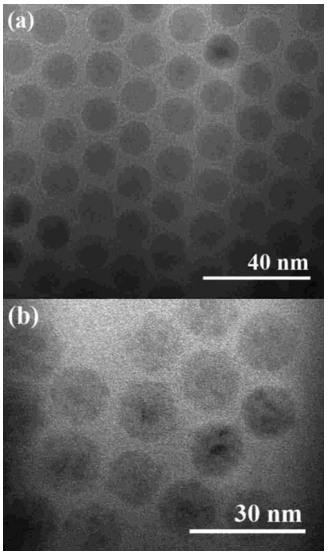

FIG. 1. (a) TEM image of ~14 nm FeO/Fe_3O_4 core-shell NCs. (b) High-resolution TEM image depicting the dimensions of core and shell.

presence of oleic acid.[17] Synthesis of the iron oleate precursor involves the reaction of 2.17 g of $FeCl_3 \cdot 6H_2O$ with 7.30 g of sodium oleate in a mixture of 16 mL ethanol, 12 mL DI water, and 28 mL hexane at 70 °C under constant stirring at 400 rpm. The iron oleate is further heated at 75 °C under vacuum for 24 h. Synthesis of 14 nm core-shell NCs is achieved by the thermal decomposition of 1.6 mmol iron oleate and 0.8 mmol oleic acid in 1-octadecene. The temperature is increased at 3 °C/min, and the solution is allowed to reflux at 320 °C for 45 min. FeO NCs are initially formed, followed by a core-shell structure of FeO/Fe_3O_4 upon exposure to air. The inverted magnetic structure is a consequence of the chemical instability of the FeO phase, which undergoes a disproportionation process to Fe_3O_4. Figure 1 depicts typical transmission electron microscopy (TEM) images of the as-synthesized core-shell NCs; a high-resolution TEM image is shown in Fig. 1(b). A variation in the structure of the AFM core is observed, with some FeO/Fe_3O_4 core-shell NCs consisting of a single core and others consisting of multiple grains of reduced size. Analysis of our TEM images yields an average core diameter of $d_C \approx 7$ nm and an average shell thickness of $t_S \approx 3.5$ nm.

III. X-RAY DIFFRACTION MEASUREMENT

Structural investigations of the FeO/Fe_3O_4 core-shell NCs are conducted by x-ray diffractometry (XRD). XRD measurements are performed using a Scintag X_1 θ/θ automated powder x-ray diffractometer, equipped with a Cu ($\lambda_{Cu}=1.5406$ Å) target and a Peltier-cooled solid-state detector. Samples are supported on zero-background Si (511) plates. The XRD spectrum of the core-shell NCs is provided in Fig. 2(a). The diffraction peaks correspond to a mixture of wüstite (FeO JCPDF #46–1312) and spinel (maghemite: Fe_2O_3 JCPDF#39–1346 and/or magnetite: Fe_3O_4, JCPDF#19–0629) phases of iron oxide. A Scherrer equation

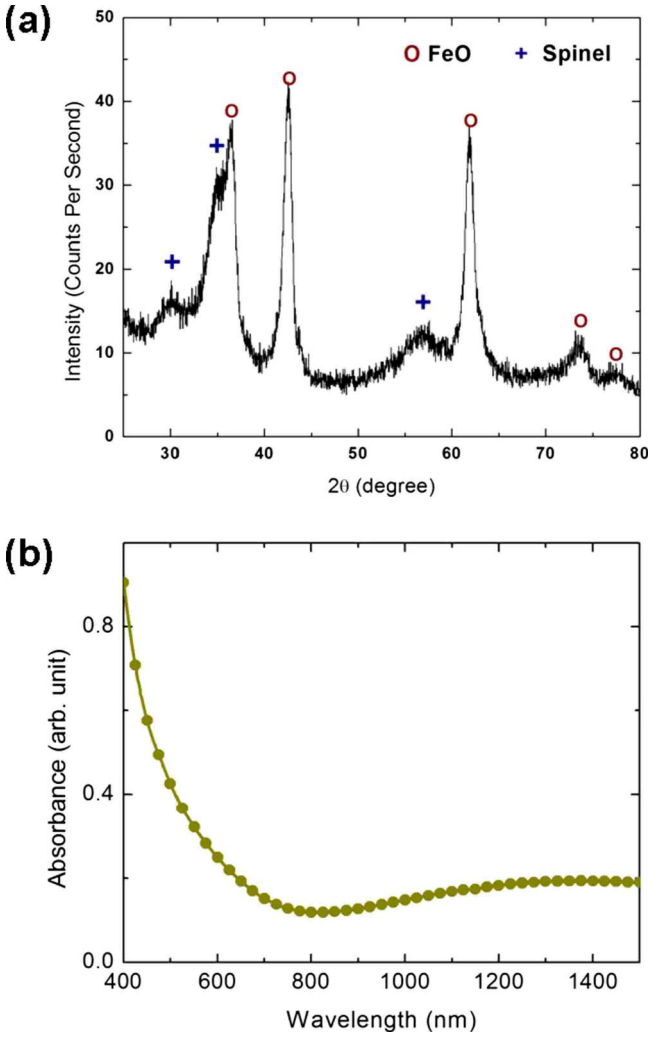

FIG. 2. (Color online) (a) XRD spectrum of as-synthesized 14 nm FeO/Fe_3O_4 core-shell NCs. The spinel peaks are symbolized by + and the wüstite peaks by O. (b) Absorption spectra of core-shell NCs dispersed in toluene. The near-IR absorption signature at approximately 1380 nm is indicative of the magnetite (Fe_3O_4) phase of iron oxide.

analysis of the peaks provides an approximate assessment of the dimension of the wüstite core. From this assessment, we determine the wüstite cores have an average diameter of $d_C \approx 8.5$ nm. This result is comparable to the wüstite core diameter obtained from the TEM analysis. Given the similar crystallinity of maghemite and magnetite, distinguishing between the phases within nanocrystallites is very difficult. Complementary absorption spectroscopy analyses can proffer additional information to facilitate a definitive identification.

IV. ABSORPTION SPECTROSCOPY MEASUREMENT

In order to distinguish between the Fe_3O_4 and Fe_2O_3 spinel phases of iron oxide, of which the shell of our NCs may consist, an absorption measurement of the core-shell NCs dispersed in toluene was performed, depicted in Fig. 2(b). The background absorption signature of the toluene solvent

was extracted from the measured absorption, leaving the absorption spectrum of the core-shell NCs alone. The primary absorption difference between Fe_3O_4 and Fe_2O_3 resides within the infrared region, where Fe_3O_4 has a prominent absorption feature at approximately $\lambda = 1380$ nm. This feature, not observed in Fe_2O_3, corresponds to the Fe^{2+}-Fe^{3+} charge-transfer transition of magnetite.[18,19]

V. EXPERIMENTAL RESULTS AND DISCUSSION

A brief review of magnetic NCs is necessary in order to describe the essential features of EB in core-shell systems. The total energy of an ensemble of single domain colloidal magnetic NCs can be described by the magnetic dipole-dipole interaction, the Zeeman energy, and the magnetic anisotropy energy. The magnetic anisotropy of a NC defines the easy direction(s) of the spin. Rotation of the spin magnetic moment along the easy axes occurs when the energy barriers are overcome. Spherical single domain NCs are considered as having uniaxial anisotropy, for which the system can be represented as having a single easy axis with a giant net spin. The uniaxial anisotropy energy is given by

$$E_A = -K_U V_i \left(\frac{\vec{\mu}_i \cdot \vec{n}_i}{|\vec{\mu}_i|} \right)^2, \tag{1}$$

where K_U is the uniaxial anisotropy constant, V_i the volume of particle i, and $\vec{n}_i$ is the direction of the easy axis of particle i. The uniaxial anisotropy constant of spherical Fe_3O_4 NCs ranges from $K_U \approx 2 \times 10^4$ J/m^3 to $K_U \approx 5 \times 10^4$ J/m^3.[20] For dilute dispersions of NCs, when the thermal energy ($k_B T$) becomes comparable to the magnetic anisotropy energy given by Eq. (1), the barrier for rotation is overcome and the giant spin fluctuates about the easy axis. In this instance, the NCs are said to be superparamagnetic since the time average of the magnetization of each particle vanishes in zero applied field. When the thermal energy is insufficient to cause a reversal of the spin on the time scale of the measurement, the spin remains fixed along the easy axis, and the NC is referred to as being blocked. The temperature at which the thermal energy induces a transition from the blocked state to the superparamagnetic state is defined as the blocking temperature (T_B^{SP}). The blocking temperature usually shifts to larger values when the magnetic dipole-dipole energy becomes comparable to the magnetic anisotropy energy.[21]

For the FeO/Fe_3O_4 core-shell NCs, the magnetic anisotropy energy of both the ferrimagnet and antiferromagnet must be considered, as well as the exchange coupling at the AFM/FIM interface. The magnetic anisotropy constant of the ferrimagnet and antiferromagnet will be distinguished by K_F and K_A, respectively. EB is generally observed in thin-film systems when $K_A \gg K_F$ and the thickness of the antiferromagnet is sufficient in size. The effective magnetic anisotropy energy in EB systems can be complex, since the antiferromagnet can induce both unidirectional anisotropy and higher-order anisotropy (e.g., uniaxial). Unidirectional anisotropy is characterized by one stable spin direction, while the uniaxial anisotropy given by Eq. (1) yields two stable spin directions. Induced anisotropy from the antiferromagnet can therefore alter the spin relaxation of the ferrimagnet with respect to the thermal energy.

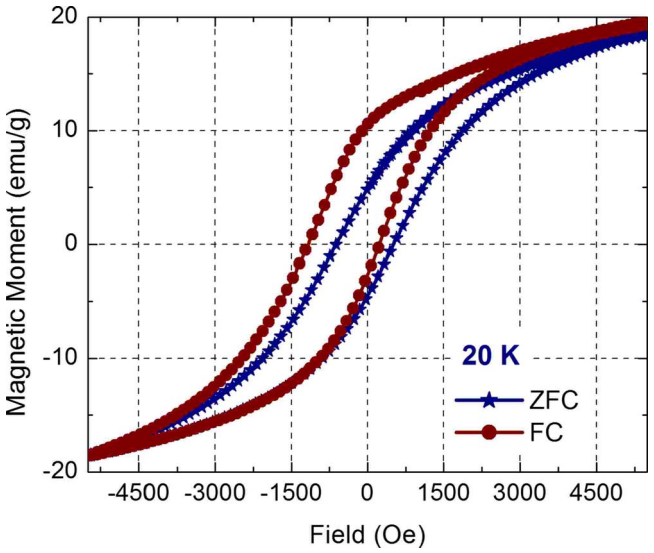

FIG. 3. (Color online) ZFC and FC measurements of $m(H)$ for 14 nm FeO/Fe_3O_4 core-shell NCs. The star curve is the ZFC hysteresis loop at 20 K. The circle curve is the FC ($H_{FC} = 1000$ Oe) hysteresis loop at 20 K. The cycling field is ± 5500 Oe.

Exchange coupling at the AFM/FIM interface of the singly inverted FeO/Fe_3O_4 core-shell NCs is investigated by the ZFC/FC measurement of $m(H)$. Figure 3 illustrates the FC ($H_{FC} = 1$ kOe) and ZFC hysteresis loops at 20 K for a cycling field of ± 5500 Oe. Closed loops are obtained for this cycling field; however, minor loop effects are still a possibility since complete saturation is not technically obtained. According to the figure, the singly inverted system exhibits the properties of an exchanged biased system, with a horizontal shift along the field axis of the FC hysteresis loop with respect to the ZFC hysteresis loop. The horizontal shift is a measure of the exchange field given by

$$H_E = \frac{-(h_+ + h_-)}{2}, \tag{2}$$

where h_- and h_+ are the points of intersection on the field axis at decreasing (−) and increasing (+) fields. The coercive field is defined by

$$H_C = \frac{(h_+ - h_-)}{2} \tag{3}$$

and is measured from the point of origin given by H_E. The FC hysteresis loop is shifted in the direction of negative field, with an exchange field of $H_E = -471$ Oe and an enhanced coercive field of $H_C = 700$ Oe. A slight positive vertical shift along the magnetization axis is also present. In AFM/FM systems, vertical shifts are generally related to pinned uncompensated spins that exhibit either FM or AFM coupling at the interface.[22,23] The positive vertical shift in Fig. 3 indicates a dominant FM coupling between the pinned uncompensated spins and the FIM magnetization.

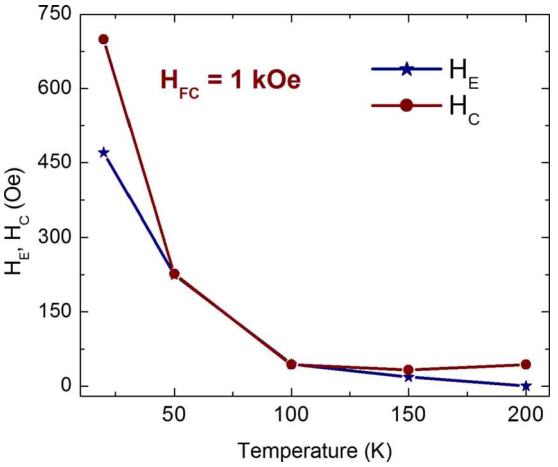

FIG. 4. (Color online) Plot of the temperature dependence of H_E and H_C. Lines connecting the data points are guides to the eyes.

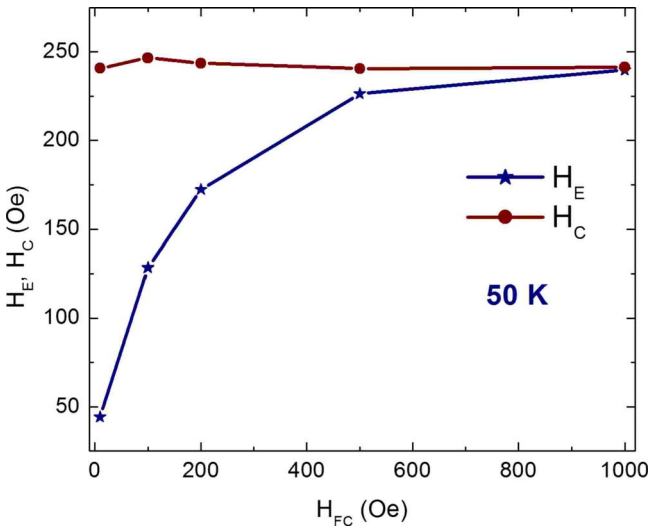

FIG. 5. (Color online) Plot of the field-cooling dependence of H_E and H_C at a constant temperature of 50 K. Lines connecting the data points are guides to the eyes.

Given that exchange coupling at the interface of core-shell NCs is dependent upon temperature, additional measurements of the FC and ZFC hysteresis loops were conducted at 50, 100, 150, and 200 K. The field-cooling parameter and cycling field are identical to the 20 K case. The temperature dependences of both H_E and H_C are plotted in Fig. 4. According to the figure, $H_E/H_C \leq 1$ for all temperatures below the blocking temperature of EB (T_B^{EB}). T_B^{EB} is determined by the temperature at which $H_E=0$ Oe. A nonlinear decrease in the exchange field is observed as the temperature is increased from 20 to 200 K. At 150 K, the magnitude of EB is significantly reduced, which is confirmed by the small exchange field ($H_E=18$ Oe). Figure 4 indicates that $T_B^{\mathrm{EB}} \approx T_N$ for the singly inverted FeO/Fe_3O_4 core-shell NCs. This behavior is in contrast to the doubly inverted MnO/Mn_3O_4 system, which displays a greatly reduced value of T_B^{EB} above 65 K, yielding a value of T_B^{EB} markedly less than $T_N \approx 118$ K.[24] Core-shell NCs without inversion of the magnetic structure often yield values of T_B^{EB} much less than T_N, since the magnetic stability and ordering of the antiferromagnet can be altered by finite-size effects.[25,26] A reduced value of T_B^{EB} with respect to T_N was reported for Co/CoO core-shell NCs by Nogués *et al.*,[27] who attributed the behavior to the thickness (~ 1 nm) of the AFM CoO shell. However, the magnetic properties of the CoO shells were recovered for particles in close contact, resulting in an increase of T_B^{EB} by nearly 2 orders of magnitude as a consequence of the increase in the effective CoO thickness. Therefore, the dimensions of the antiferromagnet in a core-shell system, as well as other parameters, must be carefully tailored in order to preserve EB at higher temperatures. Singly inverted FeO/Fe_3O_4 core-shell NCs show remarkable stability of EB, with $T_B^{\mathrm{EB}} \approx T_N$, most likely because of the large average diameter ($d_C \approx 7$ nm), crystallinity, and local environment of the AFM FeO core.

The pinning of uncompensated interfacial spins requires a relatively large AFM anisotropy of the core. According to the simplest model of EB, in reference to thin-film systems, the product of the magnetic anisotropy constant (K_A) and the thickness of the antiferromagnet must necessarily be greater than the interface exchange constant. The analog of this condition is met in the core-shell system since EB is observed up to $T_B^{\mathrm{EB}} \approx T_N$. The observation of both EB and an enhanced coercivity from the FC measurement of $m(H)$ implies a population of both pinned and unpinned uncompensated spins at the interface. Pinned uncompensated spins remain anchored to the antiferromagnet upon cycling the magnetic field and induce H_E, as observed from the shifted hysteresis loop in Fig. 3.[28] Unpinned uncompensated spins rotate with the ferrimagnet, through a spin drag effect, and result in the enhanced coercive field H_C.[29–31] Given that $H_E/H_C \leq 1$ for all temperatures below T_B^{EB}, a larger number of uncompensated interfacial spins must be unpinned, as opposed to pinned, in the singly inverted FeO/Fe_3O_4 core-shell system.

Figure 5 illustrates the dependence of H_E and H_C on H_{FC} at a constant temperature of 50 K. The cycling field is ± 5500 Oe for each value of the applied cooling field. The value of H_C remains fairly constant for cooling fields ranging from 10 to 1000 Oe. Conversely, H_E displays a strong dependence on H_{FC} in the low-field regime. A significant increase in H_E occurs as H_{FC} is increased from 10 to 500 Oe. This is most likely a result of the incomplete saturation of the FIM shell at low cooling fields. At $H_{\mathrm{FC}}=1000$ Oe, the value of H_E appears to approach a maximum value. Although not included in the present study, an investigation of the dependence of H_E and H_C on larger values of H_{FC} would be of interest. Depending upon the nature of the AFM/FIM interface, the core-shell system could display either a saturation or a decrease of H_E in the high field-cooling regime. Regarding MnO/Mn_3O_4 core-shell NCs, a saturation of H_E has been reported for cooling fields larger than 30 kOe.[8] Other systems involving a spin-glass phase exhibit a decrease in H_E for large cooling fields.[32] Setting aside this issue, it is certain from Fig. 5 that negative EB results for all cooling fields less than 1000 Oe. Additionally, a positive shift along the magnetization axis is found to increase substantially as H_{FC} increases. This is a further indication of FM coupling of pinned AFM spins with the FIM spins at the interface. Consequently, a negative horizontal shift of the FC hysteresis loop presumably persists for $H_{\mathrm{FC}} > 1000$ Oe.

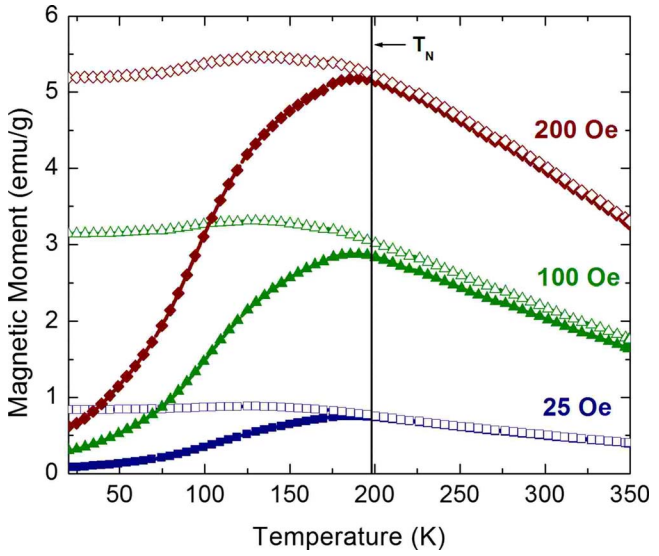

FIG. 6. (Color online) ZFC and FC measurements of $m(T)$ for 14 nm FeO/Fe_3O_4 core-shell NCs. The ZFC/FC data are given by filled/open symbols at 25, 100, and 200 Oe. The Néel temperature of wüstite is marked with a solid line at T_N=198 K.

According to the ZFC/FC measurements of $m(T)$, as plotted in Fig. 6, the FeO/Fe_3O_4 core-shell NCs exhibit superparamagnetic behavior at room temperature, with a blocking temperature of $T_B^{SP} \approx 190$ K. Using $K_U \approx 5 \times 10^4$ J/m^3 and the measured value of the shell volume from TEM, the expected $T_B^{SP} = K_U V / 25 k_B$ is approximately 180 K, assuming that the NCs are isolated from each other. Since the NC density is greater than the dilute limit, we must estimate the dipole moment in order to gauge the effect of particle interactions on the value of T_B^{SP}. To first approximation, the decay in magnetization ($T > T_B^{SP}$) is fit with the Langevin equation, yielding an average dipole moment per NC of $\mu \approx 9060 \mu_B$, where μ_B is one Bohr magneton.[33] Although the dipole moment is relatively weak, the distance between NCs is on the order of a few nanometers. Hence, the small increase in T_B^{SP} is a consequence of both dipole-dipole interactions and the induced anisotropy from the presence of the AFM core in the NC.

The most interesting result from the measurement of $m(T)$ is the weak dependence of T_B^{SP} on the applied field, the results of which are provided in Fig. 6. Unlike interacting superparamagnetic NCs, T_B^{SP} does not shift to lower temperature upon increasing the applied field from 25 to 200 Oe after cooling in zero applied field.[34] Actually, the value of T_B^{SP} increases from 188 K at 25 Oe to 190 K at 200 Oe. Hence, the value of T_B^{SP} is nearly constant for this range of applied field. Usually, an increase in the applied field tends to decrease the effective barriers to spin reorientation in weakly interacting systems, causing a monotonic decrease in T_B^{SP} as a function of the applied field.[35] Since $T_B^{SP} \approx T_N$, the weak dependence on applied field must be related to the presence of the antiferromagnet and the exchange coupling at the AFM/FIM interface. The anisotropy of only the ferrimagnet can be ruled out since the expected T_B^{SP} is lower than the measured value. In addition to unidirectional anisotropy, the AFM FeO core can induce higher order anisotropies in the FIM shell. According to Gruyters and Schmitz,[36] the simplest case involves an enhanced uniaxial anisotropy, originating from the unpinned AFM spins that rotate with the ferrimagnet. Significant modification of the spin relaxation can occur from this spin drag effect, causing a deviation from the classic Néel relaxation model. Consequently, the induced anisotropy from the antiferromagnet results in $K_U V \gg k_B T$, for $T < T_B^{EB}$. This argument was applied by Skumryev *et al.*[3] to explain the enhanced thermal stability of Co/CoO core-shell NCs. For the singly inverted FeO/Fe_3O_4 core-shell NCs, this argument also explains the stability of T_B^{SP} with respect to the applied field. The net effect is a well-defined crossover from the blocked state to the superparamagnetic state, as a result of the correlation between T_B^{SP} and T_B^{EB}.

VI. CONCLUDING REMARKS

In summary, we have investigated the EB properties of singly inverted FeO/Fe_3O_4 core-shell NCs. FC measurements of $m(H)$ confirm a negative horizontal shift along the field axis and a positive vertical shift along the magnetization axis. The blocking temperature of the exchange field is $T_B^{EB} \approx T_N$. Measurements of $m(T)$ indicate induced anisotropy in the ferrimagnetic shell, causing a crossover from the blocked state to the superparamagnetic state that is virtually unaffected by an applied magnetic field as large as 200 Oe. Investigations of other singly inverted systems, especially those consisting of an antiferromagnet with T_N above room temperature, may provide a facile route to obtaining thermally stable nanostructures for device applications.

ACKNOWLEDGMENTS

We would like to acknowledge Dmitry Koktysh for useful discussions concerning the synthesis of iron oxide nanocrystals. This work was funded by NNSA under Contract No. DE-FG 52-06NA26193, NHMFL-IHRP, NSF under Contract No. DMR-0084173, and the State of Florida.

[1] W. H. Meiklejohn and C. P. Bean, Phys. Rev. **102**, 1413 (1956).
[2] C. Chappert, A. Fert, and F. N. Van Dau, Nature Mater. **6**, 813 (2007).
[3] V. Skumryev, S. Stoyanov, Y. Zhang, G. Hadjipanayis, D. Givord, and J. Nogués, Nature (London) **423**, 850 (2003).
[4] A. E. Berkowitz and K. Takano, J. Magn. Magn. Mater. **200**, 552 (1999).
[5] J. Nogués and I. K. Schuller, J. Magn. Magn. Mater. **192**, 203 (1999).
[6] J. Nogués, J. Sort, V. Langlais, V. Skumryev, S. Suriñach, J. S. Muñoz, and M. D. Baró, Phys. Rep. **422**, 65 (2005).
[7] A. E. Berkowitz, G. F. Rodriguez, J. I. Hong, K. An, T. Hyeon,

N. Agarwal, D. J. Smith, and E. E. Fullerton, J. Phys. D **41**, 134007 (2008).
[8] G. Salazar-Alvarez, J. Sort, S. Suriñach, M. D. Baró, and J. Nogués, J. Am. Chem. Soc. **129**, 9102 (2007).
[9] H. Ohldag, A. Scholl, F. Nolting, E. Arenholz, S. Maat, A. T. Young, M. Carey, and J. Stöhr, Phys. Rev. Lett. **91**, 017203 (2003).
[10] W. Kuch, L. I. Chelaru, F. Offi, J. Wang, M. Kotsugi, and J. Kirschner, Nature Mater. **5**, 128 (2006).
[11] D. L. Peng, K. Sumiyama, T. Hihara, S. Yamamuro, and T. J. Konno, Phys. Rev. B **61**, 3103 (2000).
[12] V. Baltz, J. Sort, S. Landis, B. Rodmacq, and B. Dieny, Phys. Rev. Lett. **94**, 117201 (2005).
[13] A. Scholl, F. Nolting, J. W. Seo, H. Ohldag, J. Stohr, S. Raoux, J. P. Locquet, and J. Fompeyrine, Appl. Phys. Lett. **85**, 4085 (2004).
[14] H. Béa, M. Bibes, F. Ott, B. Dupé, X. H. Zhu, S. Petit, S. Fusil, C. Deranlot, K. Bouzehouane, and A. Barthélémy, Phys. Rev. Lett. **100**, 017204 (2008).
[15] F. X. Redl, C. T. Black, G. C. Papaefthymiou, R. L. Sandstrom, M. Yin, H. Zeng, C. B. Murray, and S. P. O'Brien, J. Am. Chem. Soc. **126**, 14583 (2004).
[16] R. J. McQueeney, M. Yethiraj, S. Chang, W. Montfrooij, T. G. Perring, J. M. Honig, and P. Metcalf, Phys. Rev. Lett. **99**, 246401 (2007).
[17] L. M. Bronstein, X. L. Huang, J. Retrum, A. Schmucker, M. Pink, B. D. Stein, and B. Dragnea, Chem. Mater. **19**, 3624 (2007).
[18] C. H. Hsia, T. Y. Chen, and D. H. Son, Nano Lett. **8**, 571 (2008).
[19] M. V. Kovalenko, M. I. Bodnarchuk, R. T. Lechner, G. Hesser, F. Schaffler, and W. Heiss, J. Am. Chem. Soc. **129**, 6352 (2007).
[20] P. C. Fannin and S. W. Charles, J. Phys. D **27**, 185 (1994).
[21] P. Allia, M. Coisson, P. Tiberto, F. Vinai, M. Knobel, M. A. Novak, and W. C. Nunes, Phys. Rev. B **64**, 144420 (2001).
[22] H. Ohldag, H. Shi, E. Arenholz, J. Stöhr, and D. Lederman, Phys. Rev. Lett. **96**, 027203 (2006).
[23] J. Nogués, C. Leighton, and I. K. Schuller, Phys. Rev. B **61**, 1315 (2000).
[24] A. E. Berkowitz, G. F. Rodriguez, J. I. Hong, K. An, T. Hyeon, N. Agarwal, D. J. Smith, and E. E. Fullerton, Phys. Rev. B **77**, 024403 (2008).
[25] C. P. Graf, R. Birringer, and A. Michels, Phys. Rev. B **73**, 212401 (2006).
[26] J. B. Tracy, D. N. Weiss, D. P. Dinega, and M. G. Bawendi, Phys. Rev. B **72**, 064404 (2005).
[27] J. Nogués, V. Skumryev, J. Sort, S. Stoyanov, and D. Givord, Phys. Rev. Lett. **97**, 157203 (2006).
[28] S. Roy, M. R. Fitzsimmons, S. Park, M. Dorn, O. Petracic, I. V. Roshchin, Z.-P. Li, X. Batlle, R. Morales, A. Misra, X. Zhang, K. Chesnel, J. B. Kortright, S. K. Sinha, and I. K. Schuller, Phys. Rev. Lett. **95**, 047201 (2005).
[29] Y. H. Chu, L. W. Martin, M. B. Holcomb, M. Gajek, S.-J. Han, Q. He, N. Balke, C.-H. Yang, D. Lee, W. Hu, Q. Zhan, P.-L. Yang, A. Fraile-Rodríguez, A. Scholl, S. X. Wang, and R. Ramesh, Nature Mater. **7**, 478 (2008).
[30] D. Givord, V. Skumryev, and J. Nogués, J. Magn. Magn. Mater. **294**, 111 (2005).
[31] P. J. Jensen, Appl. Phys. Lett. **78**, 2190 (2001).
[32] L. Del Bianco, D. Fiorani, A. M. Testa, E. Bonetti, and L. Signorini, Phys. Rev. B **70**, 052401 (2004).
[33] G. A. Held, G. Grinstein, H. Doyle, S. H. Sun, and C. B. Murray, Phys. Rev. B **64**, 012408 (2001).
[34] P. Dutta, A. Manivannan, M. S. Seehra, N. Shah, and G. P. Huffman, Phys. Rev. B **70**, 174428 (2004).
[35] M. Azeggagh and H. Kachkachi, Phys. Rev. B **75**, 174410 (2007).
[36] M. Gruyters and D. Schmitz, Phys. Rev. Lett. **100**, 077205 (2008).